Active Optics and X-Ray Telescope Mirrors

Gérard R. Lemaitre

Observatoire Atronomique Marseille Provence
38 rue F. Joliot-Curie, F-13388 Marseille CEDEX 13, EU

Keywords: Active optics, Mirror aspherization, Tubular mirrors, X-ray telescopes, Optical control.

ABSTRACT

For more than 40 years in Marseille Provence observatories active optics concepts have found many fruitful developments in uv, visible and ir telescope optics. For these wavelength ranges, active optics methods are now widely extended by current use of variable curvature mirrors, in situ aspherization processes, stress figuring apsherization processes, replications of stressed diffraction gratings, and in situ control of large telescope optics. X-ray telescope mirrors will also benefit soon from the enhanced performances of active optics. For instance, the 0.5-1 arcsec spatial resolution of Chandra will be followed up by increased resolution space telescopes which will require the effective construction of more strictly aplanatic grazing-incidence two-mirror systems.

In view to achieve a high-resolution imaging with two-mirror grazing-incidence telescope, say, 0.1 arcsec, this article briefly reviews the alternative optical concepts. Next, active optics analysis is investigated with the elasticity theory of shells for the active aspherization and in situ control of monolithic and segmented telescope mirrors for x-ray astronomy. An elasticity theory of weakly conical shells is developed for a first approach which uses a monotonic extension (or retraction) of the shell.

1. INTRODUCTION – ACTIVE OPTICS METHODS

Active optics methods have proved extremely efficient to avoid ripple errors in the aspherization process of a mirror surface. For more than 40 years in Marseille Provence observatories, active optics concepts have found many fruitful developments in uv, visible and ir telescope optics.[1,2] For these wavelength ranges, active optics methods are now widely extended by current use of variable curvature mirrors, in situ aspherization processes, stress figuring apsherization processes, replications of stressed diffraction gratings, and in situ control of large telescope optics.

Although presently unused for x-ray telescopes, active optics methods could provide soon an enhanced angular resolution imaging of the sky, say, 0.1 arcsec. The various optical designs of two-mirror Wolter Type I telescopes are briefly reviewed and the performance compared.

2. X-RAY TELESCOPE DESIGN : WOLTER TYPE I MANIFOLDS

2.1. Monolith x-ray telescopes

The Type I design by Wolter (1952) is the shortest of two-mirror systems and therefore has been extensively utilized as *x-ray telescope* for astronomy. Compared to Type II or Type III, this design is the only one where *both* mirrors provide a beam convergence; therefore the smallest graze angles are obtained which minimizes x-ray absorption. All embarked telescopes for x-ray astronomy have been built in the Wolter Type I form.

Generally the mirrors are closely joint together and their tubular substrates have axial length to mean diameter ratios L_1/D_1 and L_2/D_2 rather short, typically $L/D \lesssim 1/4$. Depending on the amount of on-axis and field aberration residuals, various designs have been developed whose mirror figures are of the following manifolds.

• PARABOLOID-HYPERBOLOID TELESCOPES (PH) : The early imaging systems were designed with grazing incidence paraboloid and hyperboloid pair. This design is free from spherical aberration – then only *stigmatic* – but field aberration remains. The telescope geometry is completely determined by the curvatures c_1, c_2, the

Schwarzschild conic constants $\kappa_1 = -1$, κ_2, and the axial separation z_{12} of the mirrors. Such was the optical design, for instance, of the HEAO-2 telescope (Einstein) and the ROSAT telescope.

• WOLTER-SCHWARZSCHILD TELESCOPES (WS) : Abbe's sine condition is strictly satisfied by the WS telescope design. This means that a ray of the axial input beam from infinity intersects its conjugate of the output beam on the Abbe sphere. The systems perfectly satisfies the *sine condition*, thus all- order spherical aberration and linear coma vanishes. The mirror figures are determined by a parametric equation set as in the Chrétien's all-order parametric representation (1922) for the two-mirror normal-incidence case. These figures were first derived in 1972 by Chase & VanSpeybroeck [3] in a study that has become a classic reference. A generalized parametric representation for WS telescopes was obtained by Saha [4] and a dedicated raytrace code for this purpose was elaborated by Thompson & Harvey.[5] Although not entering into detail, Chase & VanSpeybroeck also computed the exact figures of the two mirrors of a WS telescope showing that both grazing-incidence mirrors may have *two inflexion zones*. In a systematic study of many WS wide field telescopes, these authors showed that the effect of the field curvature is small and that the astigmatism is dominant. They derived a general relation expressing the angular resolution – blur image residuals – of a WS telescope as a function of the telescope parameters and field of view.

Because of the inflexion zones, the mirrors have been found extremely difficult to fabricate so this design was never built up to date. However, its superiority is evident for high angular resolution imaging of small FoV, say, $2\varphi_m = 5$ arcmin in diameter.

Up to now, astronomical programs for such researches have not yet been investigated.

• SPHEROID-SPHEROID TELESCOPES (SS) : The SS telescope design is optimized with mirrors whose figures are expressed by even series where some of the expansion coefficients are unrelated. This geometry – a subclass of the spheroids – was proposed by Werner [6] for wide field telescopes. The polynomial representation roughly approximate the sine condition and reduce astigmatism. Analytic representation of mirrors with the implicit quadratic form $f(z^2, r^2, z, r, a_0) = 0$ were investigated by Burrows & al.[7] and Noll & al.[8] by use of a dedicated raytrace code. Subsequently Saha & Zhang [9] investigated an SS telescope design which was called "equal curvature". The residual aberrations are balanced but coma, astigmatism and field curvature remains in low order terms.

The SS design is attractive for moderate fields of view, say $2\varphi_m \leq 20$ arcmin. The large imaging AXAF-Chandra telescope was designed in this form with a nested coaxial mirror pairs for spectroscopy. Examples of projects underway are the WFXT and XRT.

• HYPERBOLOID-HYPERBOLOID TELESCOPES (HH) : The HH telescope design is made of two consecutive hyperboloid mirrors. Proposed by Harvey & al.[10,11], this concept use of the optimization capability of conventional raytrace codes, i.e. mirror figures that are pure conicoid surfaces, so the sine condition is no longer applied. Starting from the stigmatic design of a PH telescope, the optimization process acts with the four parameters c_1, κ_1, c_2, κ_2 and also slight variations – or despaces – of the axial separations V_1F_1 and F_2V_2 (vertex to focus). In addition the axial lengths L_1, L_2 of the mirrors and their gap must be specified. Given an intermediate field angle φ_i, such that $0 < \varphi_i < \varphi_m$, for which the aberrations must be minimized, raytrace optimizations provide aberration balanced fields where both mirrors are hyperboloids.

The HH design is attractive for a wide-field, say $2\varphi_m \simeq 30$ arcmin. It implies mirrors that have simple shapes – included in the conicoid class – which thus can be readily optimized with high order corrections by the usual raytrace codes. For instance, this design has been adopted for the Solar X-ray Imager (SXI).

CONCLUSION : Because strictly satisfying the sine condition the WS telescope design provides the highest resolution imaging over a somewhat restrained FoV. For x-ray imaging of sky regions smaller than $2\varphi_m = 5$ or 7 arcmin, this design is well appropriate.

However we have seen that the aspherization may require generating mirror figures showing one or two inflexion points.

2.2. Large segmented x-ray telescope projects

Similarly as for large ground-based telescopes in the visible and ir, future large space-based x-ray telescopes will require use of segmented and active mirrors. Examples of such projects under investigation are the SXT (Hair, Stewart & al.[12]) and XEUS (Citterio, Ghigo & al.[13]).

Investigation for the active optics aspherization – by stress figuring – of the segments is considered hereafter; this is based on the presently developed elasticity theory of weakly conical shells. The required conditions allowing this process may also be partly used for in-situ active corrections.

2.3. X-ray mirrors and super-smoothness criterion

Whatever the design option of an axisymmetric two-mirror telescope, the execution of the mirrors is difficult. The *super-smoothness* of their surface is with no doubt one of the most important feature because slope errors and scattering effects may severely degrade the image quality. The x-ray energy domain is [10-0.1 keV] which corresponds in round number to the wavelength range $\lambda\lambda\,[0.2\text{-}20\,\text{Å}]$. Hence, due to the extreme difficulty in the surface testing by x-ray in a long tunnel lab, it is presently admitted that the *surface roughness* of the mirrors must *not* exceed a value of 2-3 Å.

For this reason, active optics figuring with rigid lap segments – whose curvature is constant along the mirror axial direction – would greatly improve the performance of tubular mirrors since then avoiding ripple polishing errors. Active optics aspherization can be applied either by mirror stressing or by mandrel stressing which generates a replica mirror.

The stress figuring of long rectangular mirrors is already applied to the aspherization by a perimeter distribution of the bending moments. For such x-ray mirrors, an optimal surface geometry is further achieved by *in-situ* actuators. This two-stage process is of current use in synchrotron laboratory applications. For instance, such processes applied to long rectangular mirrors were presented by Underwood & al.[14] and Fermé.[15].

The stress figuring of grazing incidence mirrors requires use of the elasticity theory of shells. Starting hereafter from investigations with the theory of axisymmetric cylindrical shells, we shall then present an appropriate theory of axisymmetric *weakly conical shells*.

3. ELASTICITY THEORY OF AXISYMMETRIC CYLINDRICAL SHELLS

3.1. Elasticity theory of thin axisymmetric cylinders

Due to the very small amount of the maximum optical sag of x-ray mirrors, we assume hereafter that the elastic relaxation process provides the complete optical sag distribution with respect to the geometry of a cylinder or a cone, both having *straight generatrices* during the stress figuring.

The elasticity theory of thin axisymmetric cylinders involves radial *extension* and *retraction* of the mid-thickness surface. Consider the static equilibrium of a cylinder element in Fig. 1.

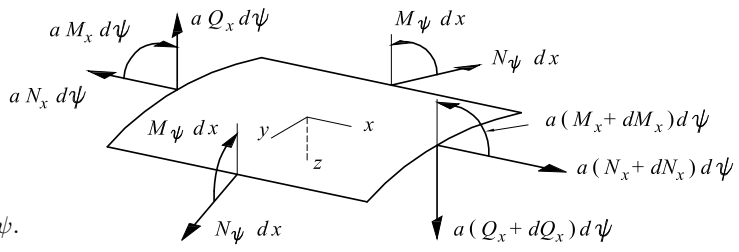

Figure 1. Static equilibrium at the mid-thickness surface of a cylinder element of lengths dx and $a\,d\psi$.

Let denote a the radius of the *middle* surface of the cylinder and q the intensity of an external uniform load, per unit area (not shown in Fig. 1), distributed all over the surface. In a small element of this surface, set an x-axis parallel to the cylinder axis and a z-axis passing through this latter axis and positive towards it. The force components involved at this element are the load q, the bending moments M_x and M_ψ, the forces N_x and N_ψ, the shearing force Q_x, and the x-variation of M_x, N_x and Q_x. From axial symmetry, the force N_ψ and the

bending moment M_ψ are constant along the circumference. Writing three equations of the static equilibrium at the center of the element – forces in x- and z-directions and flexural moment about y-axis – leads to the general differential equation of the radial flexure $w(x)$ of a cylinder of thickness $t(x)$. This equation,

$$\frac{d^2}{dx^2}\left(D\,\frac{d^2w}{dx^2}\right) \;+\; \frac{E}{a^2}\,t\,w \;=\; q, \tag{1}$$

was established around 1930 by S. Timoshenko.[16] The flexural rigidity is $D(x) = Et^3(x)/12(1-\nu^2)$ where E and ν are the Young modulus and Poisson ratio.

It is preferable to introduce a normalized variable χ instead of x. Also introducing dimensionless thickness $\mathcal{T}$ and dimensionless flexure $\mathcal{W}$, we can define these parameters as follows,

$$\chi \;=\; \Big[12(1-\nu^2)\Big]^{1/4}\,\frac{x}{a}\,, \qquad \mathcal{T} \;=\; \frac{t}{a}\,, \qquad \mathcal{W} \;=\; C\,\frac{Ew}{q\,a}\,, \tag{2}$$

where C is an unknown constant. After substitutions, we obtain a general *normalized equation of variable thickness cylinders*,

$$\frac{d^2}{d\chi^2}\left(\mathcal{T}^3\,\frac{d^2\mathcal{W}}{d\chi^2}\right) \;+\; \mathcal{T}\,\mathcal{W} \;=\; C \;\equiv\; \textit{constant}\,. \tag{3}$$

If the flexure $\mathcal{W}(\chi)$ to generate is a polynomial form, at least quadratic in χ, the integration allows deriving the radial thickness distribution $\mathcal{T}(\chi)$ from a central thickness $\mathcal{T}(0)$.

If the flexure is a constant or a linear form in χ, then the first left-hand term vanishes and the thickness distribution is either the reciprocal constant or the reciprocal linear form respectively.

3.2. Radial thickness distributions and parabolic flexure

Let consider hereafter two cases of obtaining a parabolic flexure. They are both generated by a uniform load applied all over the surface of the cylinder.

• Uniform Load in Reaction with Simply Supported Ends : A representation of a purely parabolic flexure can be simply expressed by a quadratic function of the axial ordinate as

$$\mathcal{W} \;\equiv\; C\,\frac{Ew}{q\,a} \;=\; \beta^2 \,-\, \chi^2, \qquad \chi^2 \;\le\; \beta^2, \tag{4}$$

where β is the length parameter such that $\chi = \pm\beta$ at the cylinder ends, and C is the unknown constant for the parabolic case. The radial reacting forces at the edges ensure that the radial displacement is zero at $\chi = \pm\beta$. The intensity of these two equal forces $F_\beta = F_{-\beta}$ is determined from the statics by $F_\beta + F_{-\beta} + q\,L = 0$ where $L = 2x_{\max}$ is the total length of the cylinder. One defines a *mirror aspect ratio* as

$$L/a \;=\; 2\beta/[12(1-\nu^2)]^{1/4}. \tag{5}$$

An iterative integration of (3) provide the reduced thickness $\mathcal{T}(\chi)$ as a function of the constant C, reduced thickness at the origin t_0/a, and parameter β which determines the mirror aspect ratio L/a (Fig. 2).

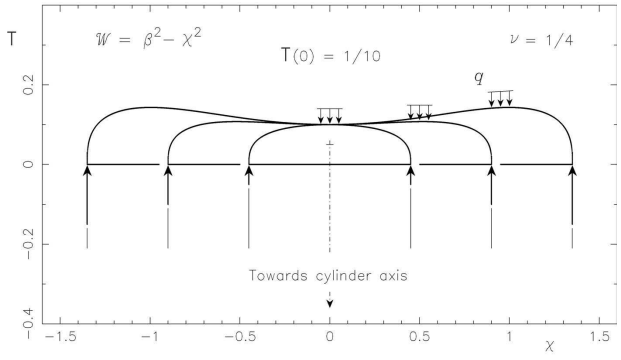

Figure 2. Thickness distributions $\mathcal{T}(\chi)$ of three cylinders generating a χ^2 flexure mode. Radial reactions at edges in equilibrium with uniform load, $F_\beta = F_{-\beta} = qL/2$. Poisson's ratio $\nu = 1/4$. Middle thickness ratio $t(0)/a = 1/10$. Length parameters $\beta = 0.45,\ 0.90,\ 1.35$. Mirror aspect ratios $L/a = 1.092\,\beta$.

The application of the radial forces at the simply supported ends requires use of axially thin collars, thus avoid any bending moment. However, even this simple boundary condition at the ends is nevertheless a practical difficulty for a mirror substrate in glass or vitro-ceram.

• Uniform Load and Free Ends – Inverse Proportional Law : Compared to the case of plane plates, an important particularity of cylinders is that edge reacting forces are not necessarily required to generate a flexure by external loads.

An axisymmetric *tubular shell* with *free edges* is by itself in a static equilibrium when a uniform load q is applied all over its surface. If no other force is applied to the shell, one shows that the shearing force Q_x vanishes. This entails that the first left-hand term in differential equation (3) also vanishes. Hence, the result is an *inverse proportional law*,

$$\mathcal{T}\,\mathcal{W} \;=\; C \;\equiv\; \textit{constant}. \tag{6}$$

→ *If an axisymmetric cylindrical shell is uniformly loaded all over one of its surfaces, and if no other external forces are applied, then the thickness $\mathcal{T}$ and flexure $\mathcal{W}$ are reciprocal functions.*

This law is of fundamental importance for the asphérization of x-ray mirrors because the boundary conditions at both edges vanish. Therefore only sliding contacts must be set at the ends to prevent from pressure leak.

1 – *Single-term parabolic flexure* : Let consider a parabolic flexure where the central section plane of the cylinder cannot extend or retract. This corresponds to a flexure $\mathcal{W}(\chi)$ and thickness $\mathcal{T}(\chi)$ with a *single* quadratic term,

$$\mathcal{W} \;=\; \chi^2, \qquad \mathcal{T} \;=\; C/\chi^2\,, \qquad \chi^2 \le \beta^2. \tag{7}$$

Hence the *thin* shell theory provides a valuable solution that is with *infinite* thickness at the plane of central section $\chi = 0$ (Fig. 3).

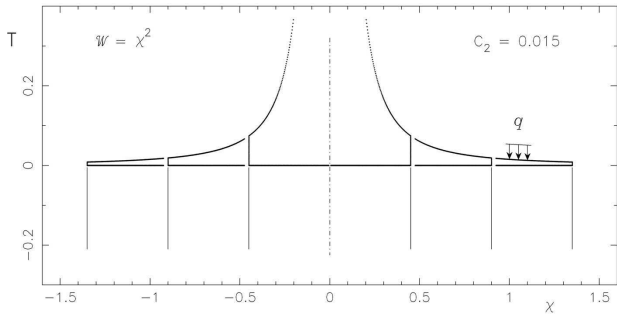

Figure 3. Thickness distribution $\mathcal{T} = C_2/\chi^2$ of three cylinders that generates a purely parabolic flexure $\mathcal{W} = \chi^2$ by uniform load only. Length parameters $\beta = 0.45,\ 0.90,\ 1.35$. Mirror aspect ratios $L/a = 1.092\,\beta$.

2 – *Two-term parabolic flexure* : The latter difficulty of an infinite thickness can be easily circumvented by considering that a radial strain may appear all along the cylinder. To generate a parabolic sag β^2 corresponding to $\beta^2 - \chi^2$, the flexure must be moved apart from zero by use of an additional constant α^2,

$$\mathcal{W} \;=\; \alpha^2 + \beta^2 - \chi^2, \qquad \chi \;=\; x/a\,, \tag{8a}$$

where the mirror aspect ratio is $L/a = 2\beta$ and the total sag of the mirror is $\mathcal{W}(0) - \mathcal{W}(\beta) = \beta^2$. From (6), the dimensionless thickness is simply the *reciprocal function*

$$\mathcal{T} \;=\; \frac{C}{\alpha^2 + \beta^2 - \chi^2}\,, \qquad \chi^2 \;\le\; \beta^2. \tag{8b}$$

The part $f(\chi) = \beta^2 - \chi^2$ must be considered as the requested flexure function representing the optical shape to generate, whilst the additional constant α^2 – which represents a *constant* retraction (or extension) along the χ-axis – is a necessary elasticity condition to avoid large or infinite thickness at any region of the cylinder. An appropriate setting of the free parameters α^2 and C provides a mirror thickness geometry that can be readily fabricated (Fig. 4).

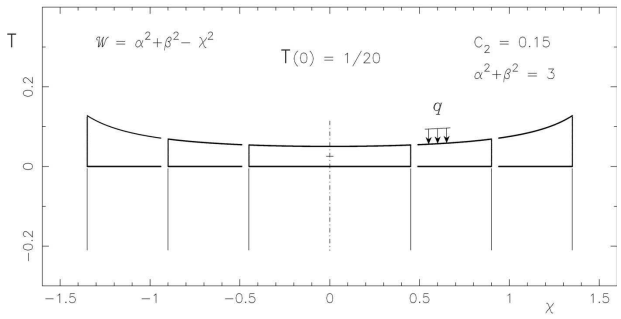

Figure 4. Thickness $\mathcal{T} = C/(\alpha^2 + \beta^2 - \chi^2)$ of three cylinders that generates a χ^2 flexure mode by uniform load only. Length parameters $\beta = 0.45$, 0.90, 1.35. Mirror aspect ratios $L/a = 1.092\,\beta$.

3.3. Radial thickness distributions and fourth-degree flexure

Fourth-degree flexures generated by a uniform load all over a shell lead to similar but more marked geometries.

• Uniform Load in Reaction with Simply Supported Edges: Similarly to the previous parabolic case, radial end forces F_β, $F_{-\beta}$ reacts to the load q. The flexure must have the form $\mathcal{W} = \beta^4 - \chi^4$, with $\chi^2 \leq \beta^2$. The thickness $\mathcal{T}(\chi)$ is derived by iterative integration. A practical difficulty is the accurate application of simply supported ends.

• Uniform Load without Reactions – Inverse Proportional Law: The *inverse proportional law* (6) applies and allow us to distinguish between the two following free end cases.

1 – *Single-term fourth-degree flexure*: A single-term flexure $\mathcal{W} = \chi^4$ leads to the thickness $\mathcal{T} = C/\chi^4$ with $\chi^2 \leq \beta^2$. One also notice that the *thin* shell theory provides a valuable solution in the form of an *infinite* thickness at the plane of central section. However this solution is mostly academic.

2 – *Two-term fourth-degree flexure*: Starting from a flexure of the form $\beta^4 - \chi^4$, the singular poles for the edge thickness, i.e. at $\chi = x/a = \pm\beta$, are avoid if the effective flexure is given an appropriate coadded constant α^2 such as $\mathcal{W} = \alpha^2 + \beta^4 - \chi^4$. Hence $\mathcal{T} = C/(\alpha^2 + \beta^4 - \chi^4)$ so the thickness geometry can be readily fabricated for glass or vitro-ceram mirrors (Fig. 5).

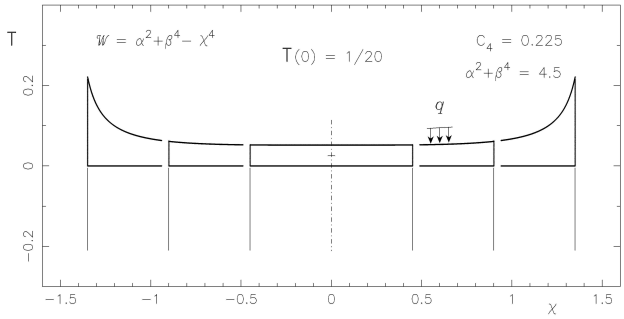

Figure 5. Thickness $\mathcal{T} = C_4/(\alpha^2 + \beta^4 - \chi^4)$ of three cylinders that generates a χ^4 flexure mode by uniform load only. Length parameters $\beta = 0.45$, 0.90, 1.35. Mirror aspect ratios $L/a = 1.092\,\beta$.

4. ELASTICITY THEORY OF WEAKLY CONICAL TUBULAR SHELLS

4.1. Flexure condition for pure extension of axisymmetric shells

In the general case of an axisymmetric two-mirror telescope, let $z(\chi)$ be a section representation of an optical surface where $\chi = x/a_0$ is an axial variable with respect to the radius a_0 of the mid-thickness of a shell at the origin $x = 0$. For instance, assume in the elastic aspherization that the figuring is conical while the mirror is under stress. The radial quantity of material $f(\chi)$ to be removed is opposite to the optical sag i.e. in the form $f(\chi) = -z(\chi) + c_1\chi + c_0$. It is natural to set the constants c_0, c_1 such that $f(\beta) = f(-\beta) = 0$ at the mirror ends, thus giving the mirror sag with respect to the cone lying to the ends. However these two conditions lead to radially unmovable ends and we have seen from the cylindrical shell theory that this entails use of radial reactions opposite to the load or infinitely thick ends. Therefore, it is preferable to consider hereafter the other alternative without any radial reaction to the load q.

If the function $f(\chi)$ is a polynomials expansion, $f(\chi) = \sum A_n\,\chi^n$, then it includes odd and even terms. We of course assume hereafter that the main *conical* term, determined by the slope of the mirror edges, is *not* obtained

by stress figuring. The general relation expressing the flexure must then writes

$$\mathcal{W} \;=\; \pm\,\alpha^2 \;+\; \sum_{n=0,1,2,3,\ldots}^{N} A_n\,\chi^n \tag{9}$$

where the constant α^2 and sign before it are set such as $\mathcal{W}(\chi)$ is with monotonic sign over the range $[-\beta,\,\beta\,]$ and never approach too closely to zero. This implies a shell in *extension condition only* – or *retraction condition only* – all over its length.

4.2. Linear product law – Relation flexure-thickness

Analysis of the deformations of a truncated weakly conical shell by either an axisymmetric linearly varying load or a uniform load – without any discrete radial circle-force except the low axial reaction R_q on the larger end – shows that there exists a simple relation between thickness and flexure. For practicable reasons, we only consider hereafter the case of a perfectly uniform external load $q = constant$.

By weakly conical shell we mean that the slope angle i of the inner surface is such as $i \leq 5°$. If t_0 and a_0 are the thickness and radius of the midthickness at $\chi = 0$, we also assume that the mirror thickness-ratio satisfies $t_0/a_0 \leq 1/10$ and that the three relations (2) applies with $a \;\rightarrow\; a_0$. Results from the elasticity theory of shells show that the relation between dimensionless thickness and flexure is the following *linear product law* [17]

$$\mathcal{T}\,\mathcal{W} \;=\; C\left(\,1 \,-\, \frac{2i}{1-t_0/a_0}\;\chi\,\right), \qquad \chi \,=\, \frac{x}{a_0} \;\in\; [\,-\beta,\beta\,]\,. \tag{10}$$

$\rightarrow$ *If a truncated weakly conical shell is radially submitted to a uniform load q all over its internal or external surface, and if no discrete circle-force is applied except the axial reaction R_q to the load, then the product thickness-flexure $\mathcal{TW}$ is a linear function of the axial coordinate χ.*

This law is of fundamental importance for the aspherization of an x-ray mirror because the shell is with both *free ends*. Thus no bending moment or radial force is needed at the boundaries except the small axial reaction R_q on the larger end which comes from the axial components of load q.

• Avoiding Poles in the Linear Product Law: For instance let assume that the flexure function $\mathcal{W}$ is represented by (9) from which the dimensioned flexure is $w = \frac{1}{C}\frac{q}{E}\,\mathcal{W}\,a_0$. Then, from the linear product law, the associated thickness is

$$\mathcal{T} \;=\; C\left(\,1 \,-\, \frac{2i}{1-t_0/a_0}\;\chi\,\right)\left(\,\pm\,\alpha^2 \,+\, \sum_{0,1,2,3,\ldots}^{N} A_n\,\chi^n\,\right)^{-1}, \tag{11}$$

For rejecting shell solutions with infinite thickness – which would also lead to a sign inversion in the load distribution q – for practice reasons, it is important to conserve a uniform load $q = constant$ and to avoid pole singularities. Since $|2i\beta/(1-t_0/a_0)| \ll 1$, this is achieved, $\forall\ \chi$, by setting a convenient value for α^2 and sign before it, in sort that $\pm\alpha^2 + \mathbf{\Sigma} A_n\chi^n$ becomes with monotonic sign over $[-\beta,\beta]$.

5. ACTIVE OPTICS ASPHERIZATION OF X-RAY TELESCOPE MIRRORS

5.1. Thickness distributions of monolithic tubular mirrors

Among the Wolter Type I telescope family reviewed in § 2.1, the Wolter-Schwarzschild (WS) form is the most performing for high angular resolution imaging in x-ray. Although limited to a few arcmin field of view, the fulfilment of the Abbe sine condition potentially allows an optical imaging towards the diffraction limited tolerance at these very short wavelengths. In counterpart, compared to the PH, SS or HH forms of this family, the shape of WS telescope mirrors is the most difficult to obtain; this fully explains why this telescope design has only been built in one or two laboratory samples (and seems to have never been used in space).

The geometry of a truncated conical shell of small slope angle for any grazing incidence mirror – hereafter simply called *tubular mirror* – can be readily determined from the linear product law.

• Linear Product Law and Tubular Mirror Design: Whatever the form of a Wolter Type I telescope – PH, WS, SS or HH forms (§ 2.1) –, relation (10) allows deriving the associated thickness distributions $\mathcal{T}_1$, $\mathcal{T}_2$ of the primary and secondary mirrors provided the flexure $\mathcal{W}_1$, $\mathcal{W}_2$ for these mirrors have been set such as the radial retraction (or extension) is always of *monotonic* sign all along the mirror surface. This is achieved by convenient choices of the α_1^2 and α_2^2 values and sign before them in (9).

• Application to Grazing Incidence WS Telescopes: As an application example of active optics asphérization, let investigate the most difficult case of WS telescope mirrors. We have seen that Chase & VanSpeybroeck [3] derived the mirror parametric representations for WS telescope (i.e. a telescope form strictly satisfying the sine condition). These authors also gave the resulting shapes for the construction and x-ray tests of a prototype WS telescope. The parameters of the primary mirror are the length $L = 165\,\mathrm{mm}$, low-angle slope corresponding to $i = 1.5°$, and inner radius $r_j = 152\,\mathrm{mm}$ at the joint of the mirrors which gives $r_0 = 154.16\,\mathrm{mm}$ at the middle of the mirror (Fig. 6).

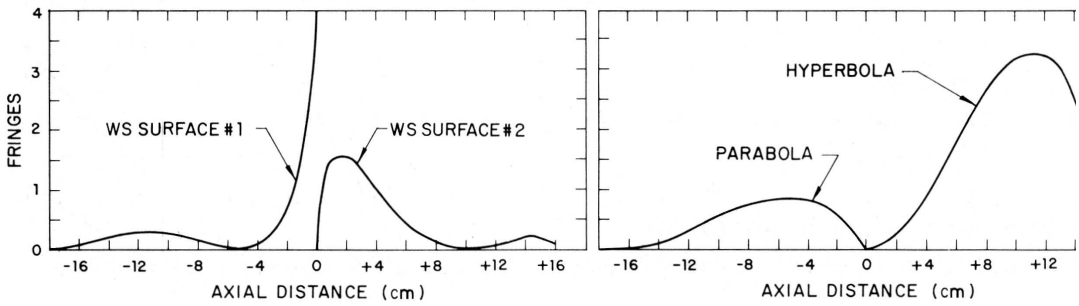

Figure 6. Mirror shapes of a WS telescope and the corresponding PH telescope from the best circles fit to each surface. One fringe is equal to one-half wavelength of 5461 Å light (after Chase & VanSpeybroeck [3]).

Using the geometrical parameters corresponding to Fig. 6 and introducing, at $\chi = 0$, a thickness $t_0 = 12.33\,\mathrm{mm}$, we obtain a central radius of the mid-surface $a_0 = r_0 + t_0/2 = 160.32\,\mathrm{mm}$ providing a shell thickness-ratio $L/a_0 = 1/13$. The edge abscissaes $\chi = \pm\beta$ is then with $\beta = L/2a_0 = 0.5146$. A polynomial representation of the WS primary mirror in Fig. 6 where $\mathbf{\Sigma}\, A_n\chi^n$ includes terms up to $n = 8$ allows to obtain, from (11), the thickness and complete geometry of this mirror when aspherized with the best circle-segment fit (Fig. 7).

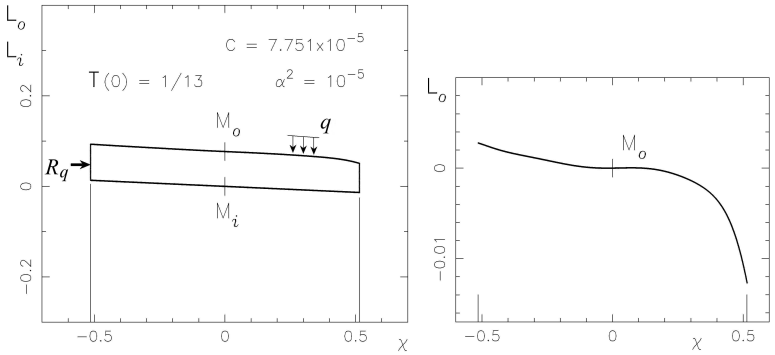

Figure 7. Shell geometry and thickness distribution of the WS primary mirror in Fig.6 aspherized by uniform load and best circle fit. [*Left*] Inner and outer lines $\mathrm{L}_i, \mathrm{L}_o$, of the shell meridian section. [*Right*] Enlarged scale of the outer line L_o after origin change and remove of the slope angle component at M_o.

In the previous example, we assumed that the aspherization is generated from the best circle-segment fit. However both curvature and aspherization can be also achieved from the best straight-segment fit. In any cases, a convenient set up of the constant α^2 and thickness $\mathcal{T}(0) = t_0/a_0$ must be done. If these two quantities are increased, then the amplitude of the outer surface with respect to a straight line is decreased, but the intensity of the load is increased.

5.2. Boundaries for segment mirrors of large tubular telescopes

Beside increasing the angular resolution of x-ray telescopes – presently limited by technological difficulties in the obtention of mirror surfaces having an extremely high smoothness –, astrophysical programs for faint object studies require the development of x-ray telescopes with much larger surface areas. Future space-based Wolter Type I telescopes will be designed with segmented mirrors allowing to construct large tubular mirrors [12,13]. The extremely high precision of the tubular surfaces to be figured and aligned will require an *extensive* use of active optics methods.

Active optics shall be mostly elaborated as well for the *stress figuring* of the sub-mirrors as for the *in situ control* of the two successive primary and secondary mirror surfaces resulting from segment assemblies.

Let consider hereafter the execution by stress figuring of a mirror segment whose contour lines are plane cuts defined by two angular planes passing through the mirror general axis and two parallel planes perpendicular to this axis. Similarly to the second deformation case of a cylinder element, we assume that the static equilibrium of the conical shell segment to a uniform load q is realized by self-compression or self-extension only, i.e. without any radial boundary forces. Then, *no* shearing force is generated through the shell, $Q_x = 0$, and the bending moments along its contour are null, $M_x = M_\psi = 0$ whatever x, ψ or χ, ψ. This means that the load q generates a *pure extension* – or a *pure retraction* – of the shell segment. Therefore, the *linear product law* (10) applies and the thickness distribution can be easily derived from this law.

For instance, when the stress figuring is operated on the inner surface of a segment by a pressure load q which acts on the outer surface of low slope angle o – which slightly differ from the inner slope angle i –, the boundaries at a segment reduce to the three following conditions (Fig. 8).

• Boundary Condition **C1**: The two facets $\pm\psi = constant$ of a segment must be supported by a normal pressure p as

$$q\, d\mathcal{A}_q\, \cos(\operatorname{atan} o) \;+\; 2p\; d\mathcal{A}_p\; \psi \;=\; 0\,, \tag{10.74}$$

where $d\mathcal{A}_q$ and $d\mathcal{A}_p$ are infinitesimal areas, of length $d\chi$, of the segment outer surface and of one of these facets. For finite values $\pm\psi$, this gives a pressure distribution $p\,(\chi) = N_\psi / t(\chi)$ which is linear only for a strictly conical thickness. However, from axial symmetry, when passing from the whole tubular cone to the segment cut, the $p\,(\chi)$ distribution in the harness support is implicitly conserved if the segment is supported by two planes passing through the mirror axis and forming a *dihedral angle* 2ψ.

• Boundary Condition **C2**: In the dihedral planes $\pm\psi = constant$, these two facets must be free to *slide* in the radial directions.

• Boundary Condition **C3**: The facet end $\chi = constant$ corresponding to the largest diameter of the loaded area must receive the axial reaction from the uniform load q. The resultant force R_q of this reaction is given by

$$q\,\mathcal{A}_q\, \sin\operatorname{atan} <o> \;+\; R_q \;=\; 0\,, \tag{10.75}$$

where $\mathcal{A}_q$ is the segment surface area receiving the load q and $<o>$ a mean-value of this surface slope angle.

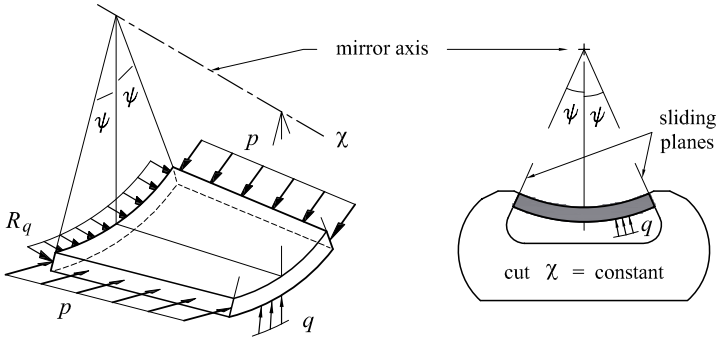

Figure 8. Equilibrium configuration for the aspherization by stress figuring and uniform loading q of a segment mirror of a large x-ray telescope. [*Left*] Force distributions for the boundary conditions **C1** and **C3**. [*Right*] Cut of a harness fulfilling those conditions and also condition **C2**.

5.3. Concluding remarks on the aspherization process and in-situ control

Compared to the aspherization of a meniscus segment for a large quasi-normal incidence telescope, the boundary conditions for a weakly conical shell are greatly simplified since the above process avoids the complication of applying perimeter bending moments.

The second stage of active optics is the in-situ control of the mirror shape. Although now actuators for bending moments may be implemented, a preferable approach would be to control the tangential stress level as a function of axial locations on the mirror or segment-mirror. This would only require simple extension or retraction wirings arranged tangentially at the opposite side of the mirror surface.

6. REFERENCES

1 G.R. Lemaitre, P. Montiel, P. Joulie, K. Dohlen, P. Lanzoni, Active optics and Modified-Rumsey wide-field telescopes: Minitrust demonstrators with vase- and tulip-form mirrors, Appl. Opt., **44**, 7322-7332 (2005)

2 G.R. Lemaitre, Active optics: vase or meniscus multimode mirrors and degenerated monomode configurations, Meccanica, Springer ed., **40**-3, 233-249 (2005)

3 R.C. Chase, L.P. VanSpeybroeck, Wolter-Schwarzschild telescopes for x-ray astronomy, Appl. Opt., **12**, 1042-1044 (1973)

4 T.T. Saha, General surface equations for glancing incidence telescopes, Appl. Opt., **26**, 658-663 (1987)

5 P.L. Thompson, J.E. Harvey, A system engineering analysis of aplanatic Wolter Type I x-ray telescopes, Opt. Eng., **39**, 1677-1691 (2000)

6 W. Werner, Imaging properties of Wolter Type I telescopes, Appl. Opt., **16**, 764-773 (1976)

7 C.J. Burrows, R. Burg, R. Giacconi, Optimal grazing incidence optics and its application to wide-field imaging. Astrophys. J., **392**, 760-765 (1992)

8 R.J. Noll, P. Glenn, J.F. Osantowski, Optical surface analysis code (Osac), in *Scattering in Optical Materils II*, S. Mussikant edt., Spie Proc., **362**, 78-82 (1983)

9 T.T. Saha, W. Zhang, Equal-curvature grazing incidence x-ray telescopes, Appl. Opt., **42**, 22, 4599-4605 (2003)

10 J.E. Harvey, A. Krywonos, P.L. Thompson, T.T. Saha, Grazing incidence hyperboloid-hyperboloid designs for wide-field x-ray imaging applications, Appl. Opt., **40**, 136-144 (2001)

11 J.E. Harvey, M. Atanassova, A. Krywonos, Balancing detector effects with aberrations in the design of wide-field grazing incidence x-ray telescopes, Opt. Eng., **45**, issue N. 6 (2006)

12 J.H. Hair, J. Stewart & al., Constellation-x soft x-ray telescope segmented optic assembly and alignment implementation, Spie Proc., **4851** (2002)

13 O. Citterio, M. Ghigo & al., Large-size glass segments for the production of the Xeus x-ray mirrors, Spie Proc., **4815** (2003)

13 J.H. Underwood, P.C. Batson, H.R. Beguiristain, E.M. Gullikson , Elastic bending and water-cooling strategies for producing high-quality synchrotron-radiation mirrors (Laurence Berkeley Nat. Lab.), Spie Proc., **3152**, 91-98 (1997)

14 J-J. Fermé, Improvement in bendable mirror polishing for x-ray optics, Société Européenne de Systèmes Optiques (Seso Corp.), Spie Proc., **3152**, 103-109 (1997)

16 S.P. Timoshenko, S. Woinowsky-Kieger, *Theory of Plates and Shells*, McGraw-Hill Book Company, New-York, 2nd issue, p. 468 (1959)

17 G.R. Lemaitre, *Astronomical Optics and Elasticity Theory*, Springer (to be published in December 2008)